Proceedings of the 17th World Congress
The International Federation of Automatic Control
Seoul, Korea, July 6-11, 2008

Reference tracking versus path-following for a one-link flexible robot manipulator

Pedro Pires   Jorge Martins   José Sá da Costa

IDMEC/IST, TULisbon Av. Rovisco Pais
1049-001 Lisboa, Portugal
e-mail: pedropires@ist.utl.pt
{martins, sadacosta}@dem.ist.utl.pt

Abstract: This paper details two control approaches for a flexible manipulator system, where the non-minimum phase problem is treated. In the first approach, we use the motion planning technique. It searches for proper output trajectories with polynomial form, in order to cancel the effects of the unstable zeros. The second approach is called Path-Following with internal model control. Its primary objective is to steer a physical object to converge to a geometric path, and its secondary objective is to ensure that an object's motion along the path satisfies a given dynamic specification.

Keywords: Flexible manipulator robot, Motion planing, Path-Following, Internal model control, Vibration control.

1. INTRODUCTION

For a long time there has been a standing interest into the use of light and flexible manipulator robots. Amongst the many improved characteristics when compared to rigid robots, perhaps the most appealing one is the higher operation speeds achievable. Unfortunately, the dynamic system of this kind of robots is of high dimension due to the links flexibility, and the control problem that is posed is a non-colocated one, since we apply torque at one end and measure position at the other end of a flexible element. This characteristic makes the control of flexible manipulators one of the areas under great investigation in robotics. The three main objectives in the control of the flexible robot arms are:

- O1 - Point to point motion of the end-effector.
- O2 - Trajectory tracking in the joint space(tracking of a desired angular trajectory).
- O3 - Trajectory tracking in the operational space (tracking of a desired end-effector trajectory).

When comparing flexible manipulators with rigid manipulators, the control methodology differs. Using rigid manipulator robots, we can achieve excellent control using simple linear joints controllers, such as Proportional-Integral-Derivative (PID) controllers. On the other hand, when we use a flexible manipulator, we have to consider the oscillations that appear at the tip during motion, therefore, we need to design a controller that contemplates feedback of the end-effector position. There are many references in the literature dealing with Non-Minimum phase systems controllers. Isidori [1999] presented a stabilization via output feedback and Dačić [2005] presented three distinct approaches for tracking in the presence of unstable zeros dynamics. He referred to them as: the Internal Model approach, the Flatness approach and the Inversion approach. Also Aguiar et al. [2004, 2005c,a], Aguiar [2005b], Aguiar and Hespanha [2007] presented the path-following methodology with an internal model control in order to control a vehicle with unstable load at a constant speed. There are less publications referring to robotic manipulator path-following. Skjetne [2005] presents the problem of a robotic cutting tool where the control objective is for the tip of the tool to trace a desired repeatable path at a constant nominal speed. Benosman and Vey [2003, 2000a,b], Benosman et al. [2002] made a profound analysis about stable inversion approach in order to cancel the unstable zero dynamics. In this paper we will mainly focus into the Internal Model Approach and the Inversion approach.

This paper is organized as follows: Section 2 recalls the dynamic equations of a flexible link. In section 3 the trajectory planning method is presented. Section 4 presents the path-following controller. The simulation results are shown in section 5, and finally the conclusions are presented in section 6.

2. DYNAMIC EQUATIONS

The research presented is based on the one joint planar flexible robot represented in figure 1. It will be considered

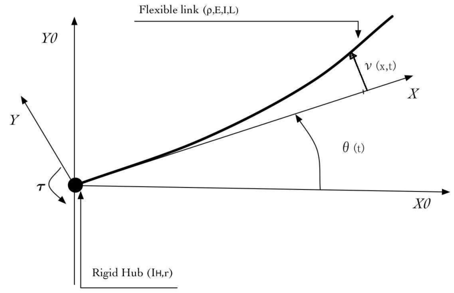

Fig. 1. Mechanical model of a single flexible link

that the flexible link is clamped to a rigid hub with a moment of inertia (I_H), radius (r) and an input torque (τ). Martins et al. [2002], Martins et al. [2003] and Martins et al. [2005] describes how to obtain the ordinary differential equations of the current system in the form

$$M\ddot{q} + Kq = T$$

where M is the system inertia matrix, K is the system stiffness matrix, T is the vector of external forces and q is the vector of generalized coordinates.

$$q = [\theta\ \eta_1\ \eta_2]^T$$
$$T = [\tau\ 0\ 0]^T$$

Here, η_i is the nodal amplitude of the ith clamped-free mode considering the assumed modes discretisation procedure. In this paper it will be considered only the first two clamped-free modes.

Considering linear displacements, the displacement at distance x from the frame origin into the OX direction, can be described as:

$$y\left(x,t\right) = x\,\theta\left(t\right) + \nu\left(x,t\right) \tag{1}$$

The total displacement is a function of the rigid body motion $\theta\left(t\right)$ and elastic deflection $\nu\left(x,t\right)$ where

$$\nu(x,t) = \sum_{i=1}^{2} \phi_i\left(x\right)\eta_i\left(t\right)$$

$\phi_i\left(x\right)$ and $\eta_i\left(t\right)$ represent the modal functions and modal amplitudes of the ith clamped-free mode respectively. The modal functions considered are

$$\phi_1\left(x\right) = 3\left(\frac{x}{L}\right)^2 - 2\left(\frac{x}{L}\right)^3$$
$$\phi_2\left(x\right) = \left(\frac{x}{L}\right)^2 - \left(\frac{x}{L}\right)^3$$
$$\phi\left(x\right) = \left[\,\phi_1\left(x\right)\ \phi_2\left(x\right)\,\right]$$

where L is the total beam length.

3. MOTION PLANING - STABLE INVERSION METHOD

We consider a non-minimum phase linear system represented in the following form,

$$P(\frac{d}{dt})u(t) = Q(\frac{d}{dt})y(t) \tag{2}$$

where P and Q are polynomials in a differential operator d/dt, with degrees m and n respectively ($m < n$). In a first analysis, the solution of (2) is composed by two terms: the transient and the steady-state.

Since system (2) has a non-minimum phase characteristic, the transient conditions contains divergent terms, as a result of the unstable zeros. Thus, the solution Benosman and Vey [2003, 2000a,b] presented is to plan the output trajectory in a way that the undesirable response of the system is cancelled considering a polynomial in time form for the output trajectory,

$$y_d = \sum_{i=1}^{p} a_i t^{i-1} \tag{3}$$

where the degree of the polynomial form p depends of the number of output initial and final constraints, as well as the number of unstable zeros associated to (2). Solving (2), we obtain $u(t) = u_t(t) + u_p(t)$ where u_t is the transient solution of the homogeneous differential (2), and u_p is the one particular solution of the inverse system.
The transient solution can be represented by:

$$u_t(t) = \sum_{i=1}^{m} A_i(a_i, t_0, u_0^{(1)}, ..., u_0^{(n-1)}) \exp^{r_i, t_i} \tag{4}$$

Where the r_i are all the roots of the characteristic equation. The A_i are linear functions of a_i coefficients and all initial conditions. It can be shown that their general expression is

$$A_i = u_0 + \sum_{j=1}^{p} \frac{a_j}{zero_i^j} \tag{5}$$

Furthermore, particular solution can be represented by:

$$u_p(t) = \sum_{i=1}^{p} B_i(a_i)t^{i-1} \tag{6}$$

To cancel the effect of the unstable zeros on the transient solution (4), (all the zeros on the right half plane or pure imaginary zeros), the A_i associated to the unstable zeros must be equal to zero.

$$A_i(a_i, t_0, u_0^{(1)}, ..., u_0^{(n-1)}) = 0 \tag{7}$$

With the previous constraint in the linear system above we can obtain the output coefficients (a_i). Just adding the final and initial constraints, this leads to the next linear system:

$$\begin{cases} A_i(a_i, t_0, u_0^{(1)}, ..., u_0^{(n-1)}) = 0 \\ y_d^i(t_0) = \text{initial conditions} \\ y_d^i(t_f) = \text{final conditions} \end{cases} \tag{8}$$

where i is the highest order for the specified output derivatives. From (8) we have the coefficients a_i and the necessary output to cancel the unstable zeros. So, the result of the remaining stable Ai is known. To complete the desired input $u(t)$, it is only necessary to obtain the particular input solution (6). The Bi elements are obtained as linear functions of the output coefficients ai, through substitution of (4) into the differential equation (2). Now, all necessary elements to obtain the desired input on an open loop form is:

$$\begin{aligned} u_{ol} = &\sum_{i=1}^{p} B_i(a_i)t^{i-1} + \\ &+ \sum_{i=1}^{m} A_{ist}(a_i, t_0, u_0^{(1)}, ..., u_0^{(n-1)}) \exp^{r_{ist}, t_i} \end{aligned} \tag{9}$$

where r_{ist} and A_{ist}, are the stable zeros and the corresponding Ai terms respectively. On a final approach to the problem, it is recommended to close the loop around the joint position in order to bring some robustness. The final closed-loop control is:

$$u_{cl}(t) = u_{ol}(t) + k\left(e_\theta, e_\theta^1, \ldots, e_\theta^{n-1}\right)^T \tag{10}$$

where the error is $e_\theta(t) = \theta_d(t) - \theta(t)$.

3.1 Example of implementation

A dynamic model from one link flexible arm with the following properties, with two bodies will be considered:

- The first one is a rigid hub with a $R = 0.075m$ radius.
- The second body is a flexible link with length of $L = 0,5m$.

The system transfer function is

$$\frac{y}{\tau} = \frac{92.5s^4 + 8.545 \times 10^{-12}s^3 - 4.924 \times 10^6 s^2 - }{s^2(s^4 + 1.066 \times 10^{-14}s^3 + 56780s^2 + } \frac{-3.015 \times 10^{-7}s + 1.163 \times 10^{10}}{+5.795 \times 10^{-10}s + 1.307 \times 10^8)} \tag{11}$$

For simplification we will call the coefficients of the numerator as a vector N, and the coefficients of the denominator as a vector D. The transfer function zeros are:

$s_{1,2} = \pm 225,2893 \qquad s_{3,4} = \pm 49,7712$

We have two unstable zeros.

The differential equation representing (11) is

$$\sum_{i=1}^{5} N(i)\tau^{(5-i)}(t) = \sum_{j=1}^{7} D(i) y^{(7-j)}(t) \tag{12}$$

associated to the initial conditions:

$$\begin{cases} \tau^{(i)}(0) = 0, & i \in \{0,1,2,3\} \\ y^{(j)}(0) = 0 & j \in \{0,1,2,3,4,5\} \end{cases}$$

As shown previously, the obtained input-output equation can be associated to any initial conditions. In this case we set the initial conditions to zero. The output that will cancel the unstable zeros must be found. The result $p = 12$ is obtained (2 unstable zeros plus 4 initial conditions on τ plus 6 initial conditions on y) where y_d from (3) must satisfy 12 constraints:

- The indices A_i corresponding to the unstable zeros
- Initial and final conditions.

$$\begin{array}{l} A_k = \tau_0 + \sum_{j=1}^{p} \frac{a_j}{Zo_k^j} = 0 \\ y^i(0) = 0 \qquad i \in \{0,1,2,3\} \\ y^i(t_f) = y_f \\ y^i(t_f) = 0 \qquad i \in \{1,2,3,4,5\} \end{array}$$

The variable Zo_k^j represents the k^{th} unstable zero powered to j. Note that these conditions were chosen to force the desired torque to be simetric. The desired a_i coefficients are then directly obtained, solving the linear system above. In this way it is possible to calculate the transient solution of the system (4). The next step is to obtain the particular solution of the system (6). The coefficients B_i's are obtained as a linear functions of the output coefficients a_i substituting equation (6) and equation (3) into equation (12). As introduced in section 3, equation (10), in order to bring some robustness to this control, a close-loop form should be used. Two types were chosen.

(1) A partial state feedback, based on the joint position and velocity variables.

$$T_{cl} = T_{ol} + K_p(\theta_d(t) - \theta(t)) + K_v(\dot{\theta}_d(t) - \dot{\theta}(t))$$
$$K_p > 0, \qquad K_v > 0$$

(2) An open loop form where the input of the system is the angle of the joint.

4. PATH-FOLLOWING FOR ONE LINK NON-MINIMUM PHASE ROBOT

The objective of the Path-Following method is to force the non-minimum phase system output to follow a geometric path without a timing law assigned to it. The systems with unstable zero dynamics have limited tracking capabilities. The only way to solve this performance limitation is to change the input-output structure of the system. This structure can be changed by reformulating the problem as path-following, rather than reference tracking. With this reformulation, it is possible to add a new timing law $\gamma(t)$ that becomes an additional control input.

In this section we define the Path-Following problem, called Internal model control, and it has the goal to achieve asymptotic tracking of reference signals, as it is demonstrated by Aguiar et al. [2005a]. The controller that incorporates an internal model of the exosystem is capable to ensure an asymptotic convergence of the tracking error to zero for every possible reference signal generated by the exosystem. The following linear time-invariant system is assumed:

$$\begin{array}{ll} \dot{x}(t) = Ax(t) + Bu(t) & x(t_0) = x_0 \\ y(t) = Cx(t) + Du(t) & \end{array} \tag{13}$$

where $x(t)$ is the state, $u(t)$ the input, and $y(t)$ the output. The main objective of this method is to reach and follow a desired geometric path $y_d(\gamma)$. The geometric path $y_d(\gamma)$ can be generated by an exosystem of the form:

$$\begin{array}{ll} \frac{d}{d\gamma} w(\gamma) = S \times w(\gamma) & w(\gamma_0) = w_0 \\ y_d(\gamma) = Q \times w(\gamma) & \end{array} \tag{14}$$

where $w \in \mathbb{R}^{2n}$ is the exogenous state and $S + S' = 0$. For any timing law $\gamma(t)$, the Path-Following error can be defined as $e(t) = y(t) - y_d(\gamma(t))$. The path $y_d(\gamma)$ is described in more detail in Pires [2007]. The following problems can be associated to the Path-Following methodology:

Geometric Path-Following: For the desired path $y_d(\gamma)$, it is necessary to design a controller that achieves:

- Boundedness: the sate $x(t)$ is uniformly bounded for all $t \geqslant t_0$, and every initial condition $(x(t_0), w(\gamma_0))$, $\gamma_0 = \gamma(t_0)$.
- error convergence: the path- following error $e(t)$ converges to zero as $t \to \infty$.
- forward motion: $\dot{\gamma}(t) > c$ for all $t \geqslant t_0$, where c is a positive constant.

Speed-assigned Path-Following: Given a desired speed $v_d > 0$, it is required that $\dot{\gamma} \to v_d$ as $t \to \infty$.

As demonstrated by Aguiar et al. [2005a] and Aguiar [2005b], we can always assume a small L_2-norm of the path following error,

$$J = \int_0^\infty \|y(t) - y_d(t)\|^2 dt = \int_0^\infty \|e(t)\|^2 dt < \delta$$

that verifies a δ arbitrarily small in order to consider a perfect tracking problem.

4.1 Controller Design - Internal model control

Aguiar et al. [2005a] presented one solution to achieve path controller for (13), such that the closed loop state is bounded. If (A, B, C, D) is a non-minimum phase system, the pair (A, B) is stabilizable, the pair (C, A) is detectable, the number of inputs is as large as the number of outputs and the zeros of (A, B, C, D) do not coincide with the eigenvalues of S (14). Then for the geometric Path-

Following problem there are constant matrices K and L, and a timing law $\gamma(t)$ such that the feedback law is:

$$u(t) = Kx(t) + L(\dot{\gamma}_d)w(\gamma(t)) \tag{15}$$

To calculate the matrices K and L, the following internal model approach is considered :

$$\begin{aligned} v_d \Pi S &= A\Pi + B\Gamma \\ 0 &= C\Pi + D\Gamma - Q \end{aligned} \tag{16}$$

As shown before, the Sylvester equations (16), are solvable if the system (A, B, C, D) is right-invertible and its zeros do not coincide with the eigenvalues of $v_d S$. The methodology to solve this equation is described as follows:

- Transform the system (16) matrices into the following system:

$$NewA = \begin{bmatrix} Kron\left(I\left(n_s\right), A\right) - Kron\left(S', I\left(n_a\right)\right) \\ Kron\left(I\left(n_s\right), C\right) \end{bmatrix.$$
$$\left. \begin{matrix} Kron\left(I\left(n_s\right), B\right) \\ Kron\left(I\left(n_s\right), D\right) \end{matrix} \right] \tag{17}$$
$$NewB = \begin{bmatrix} 0 \\ Q \end{bmatrix}$$

Where n_s is the size of the square matrix S, n_a is the size of the square matrix A, and I the identity matrix.

- From equation (17) and (16) the following formula is obtained:
$$[\,\Pi\ \Gamma\,]^T = [NewA]^{-1}[NewB]$$
- Since we now have all Π and Γ it is possible to obtain the controller gains K and L. K is calculated by a minimum quadratic regulator, that minimizes the quadratic cost function,
$$J(u) = \int_0^\infty \left(x^T Q x + u^T R u + 2x^T N u\right) dt$$
and L is equal to $L = \Gamma - K \times \Pi$.

Now that the path controller design is complete, a evolution rule to γ has to be created, in a way that, $\lim_{t\to\infty} \gamma = \gamma_d$ and $\lim_{t\to\infty} \dot{\gamma} = v_d$.

5. SIMULATION RESULTS

In this section we report some simulation results on the IST flexible arm described on figure 1.

5.1 Motion Planing - Control where the input is the torque

The method was solved for $t_f = 2.7s$ and $y_f = -0.35m$. The closed loop control was obtain using $K_p = 4$ and $K_v = 0.03$. In figures 2 and 3 we presented the simulation tracking error and the corresponding deformation of the end-effector. After a brief analysis, it is visible that the stationary error is equal to $2.5 \times 10^{-7}m$, and the vibration on the end effector is about $2 \times 10^{-7}m$. Those are very small values comparing to the obtained during the path evolution. Furthermore the error verified in figure 2 is due to the fact that the simulated model is quadratic in deformation Martins et al. [2002]. Figure 4 presents the output torque of close-loop controller. In this figure, the torque appears with small differences from the desired, due to the addition of the tracking error. The minor oscillation occurring in the steady state ($t >$ 2.5s in fig. 2), are also due to the quadratic terms of the simulated system.

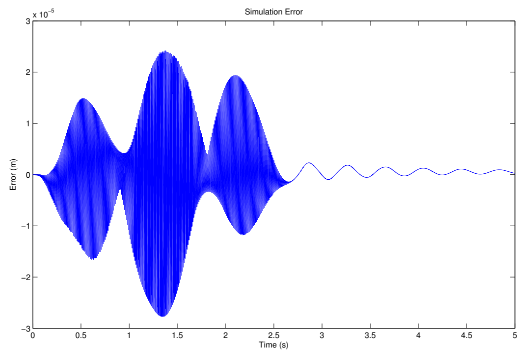

Fig. 2. Simulation tracking error

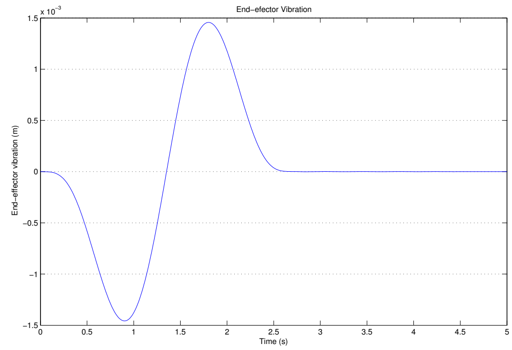

Fig. 3. Simulated end-effector deformation

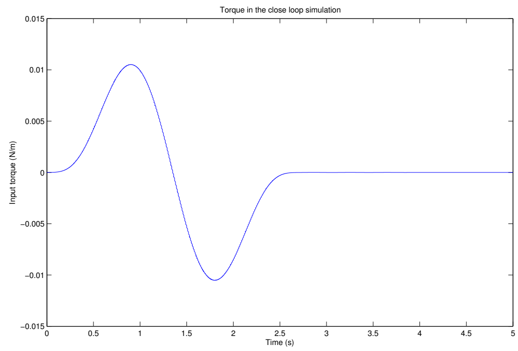

Fig. 4. Simulated close-loop torque

5.2 Control where the input of the system is the angle of the joint.

In this type of controller, the main idea is to make the system robust to external factors such as friction. Instead of calculating the transfer function between the torque and the position of the end-effector, the transfer function between the angle of the joint and the position of the end-effector has been calculated.

$$\frac{y}{\theta} = \frac{1330s^4 + 1.398 \times 10^{-9}s^3 - 7.079 \times 10^7 s^2 +}{s^6 + 334.3s^5 + 7.198 \times 10^7 s^4 + 1.456 \times 10^7 s^3 +}$$
$$\frac{+7.493 \times 10^{-5}s + 1.672 \times 10^{11}}{7.925 \times 10^8 s^2 + 6.393 \times 10^9 s + 2.907 \times 10^{11}}$$

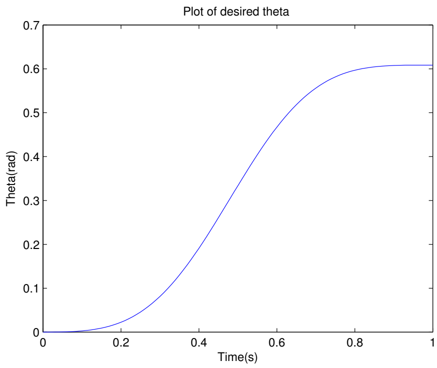

Fig. 5. Desired θ

Calculating the desired angle in a way that the undesired transient response is eliminated, the angles shown in figure 5 are obtained. By observing figure 6 and 7, we notice that the stationary error has been reduced to an insignificant value. Using this controller the system has become more robust to external factors, such as joint friction, and reduces the vibration in the steady state.

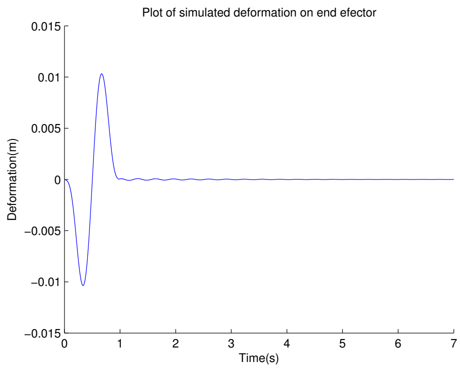

Fig. 6. Simulated end-effector deformation

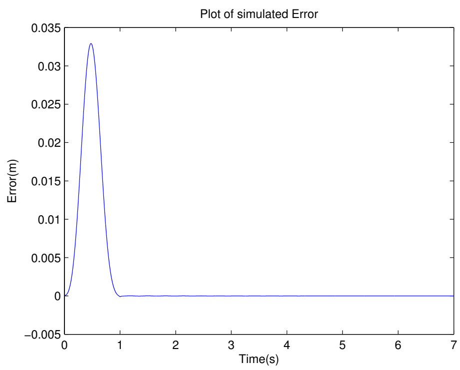

Fig. 7. Simulated error

5.3 Path-Following results

The variable y_d was used as a desired path output. The path used was:

$$
\begin{aligned}
y_d &= \left(1 - e^{(-w_d \times \gamma)} \times (1 + w_d \times \gamma)\right) y_f \\
\frac{dy_d}{d\gamma} &= \left(w_d e^{(-w_d \times \gamma)} \times (1 + w_d \times \gamma) - w_d e^{(-w_d \times \gamma)}\right) y_f \\
\frac{d^2 y_d}{d\gamma^2} &= \left(-w_d^2 e^{(-w_d \times \gamma)} \times (1 + w_d \times \gamma) + 2 w_d^2 e^{(-w_d \times \gamma)}\right) y_f
\end{aligned} \tag{18}
$$

where the variable w_d and y_f sets the convergence velocity of the system to the final value y_f. For the results presented in the next section, the following data was used. The system state space representation in continuous form is:

$$
A = \begin{bmatrix} 0 & 0 & 0 & 0 & 16040.41 & 9038.62 \\ 0 & 0 & 0 & 0 & 1143.68 & 2422.93 \\ 0 & 0 & 0 & 0 & -81331.5 & -57923.19 \\ 1 & 0 & 0 & 0 & 0 & 0 \\ 0 & 1 & 0 & 0 & 0 & 0 \\ 0 & 0 & 1 & 0 & 0 & 0 \end{bmatrix} \tag{19}
$$

$$
B = [\,607.9 \; -296.4 \; -364.7 \; 0 \; 0 \; 0\,]^T
$$

$$
C = [\,0 \; 0 \; 0 \; 0.575 \; 1 \; 0\,], \quad D = [0]
$$

where in this representation, the states are represented in the following way

$$
q = \left[\dot{\theta}, \dot{\eta}_1, \dot{\eta}_2, \theta, \eta_1, \eta_2\right]^T
$$

The variable θ represents the joint angle. For the controller calculus we used the Matlab LQR command, which requires the matrix A and B (19) and result in the following gain state space matrix

$$
\begin{aligned}
K = [\, & -10.2518 \;\; -16.8531 \;\; -2.3238 \;\; -181.8310 \\
& -126.2391 \;\; 8.1224\,]
\end{aligned} \tag{20}
$$

The value of the controller L (15) is calculated for different values of speed assignments between $0m/s$ and $5m/s$. The five seconds simulation has $y_f = \pi/8$ as final value. The path simulation has the following properties:

- A final y value $y_f = \pi/8$ in a five seconds simulation
- ω_d equal to 20.

In figure 8 we present the desired y_d versus the γ variable.

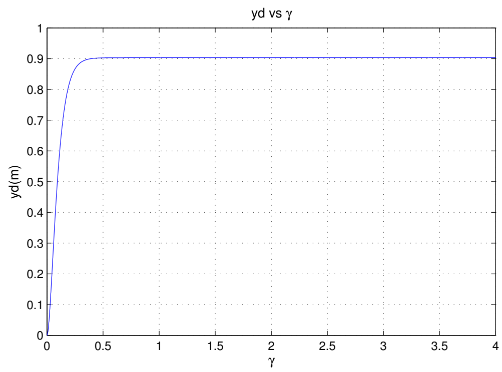

Fig. 8. Evolution of the desired output versos the path variable

Figures 9 and 10 present the simulation tracking error and the corresponding deformation of the end-effector. The tracking error and the end-effector deformation converge to zero value, as expected.

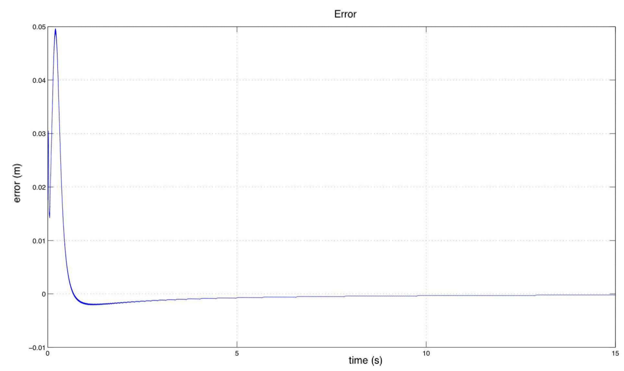

Fig. 9. Simulation Tracking error

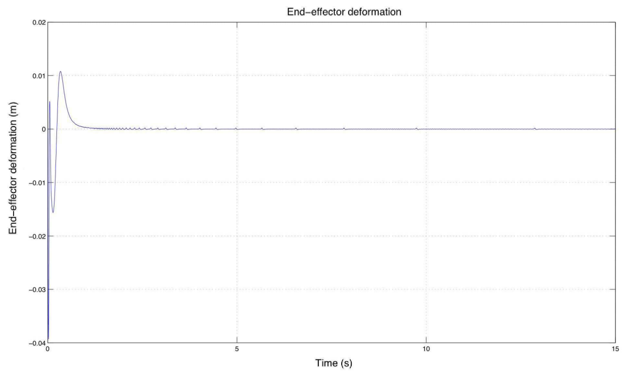

Fig. 10. Deformation of the end-effector

6. CONCLUSIONS

The stable inversion method is a simple and efficient control methodology, where all the computational effort is made offline. Regarding the control where the input of the system is the angle of the joint, it is evident that this kind of control is more robust and efficient than the control where the input is the torque. Thus, this is the controller recommended for experimental applications, due to joint friction.

Path following is still under intensive study, but the present results show its applicability to flexible manipulators. Since the reference-tracking controller is an open-loop controller respect to the tip, when the reference achieves the final value, the controller becomes passive and it does not observe the end-effector deflection, resulting on a permanent vibration. The path-following ability to separate the dynamic follower controller from the states boundedness controller, improves the control actuation. Even when the system reaches to the final value, it still removes the external perturbation. It becomes clear that the path-following controller is a much more developed and robust controller than the reference tracking controller.

ACKNOWLEDGEMENTS

This work was funded by FCT-Fundação para a Ciência e a Tecnologia, through project PTDC/EME-CRO/72085/2006, under POCI 2010, subsidized by FEDER

REFERENCES

A. P. Aguiar. Performance limitations in reference-tracking and path-following. In 44th IEEE Conference on Decision, Control, and European Control Conference Workshop, editors, *New Deveolpments in Control Performance Limitation Research: A tale in Network Age*, Seville, Spain, December 2005b.

A. P. Aguiar and J. P. Hespanha. Trajectory-tracking and path-following of underactuated autonomous vehicles with parametric modeling uncertainty. *IEEE Transactions on Automatic Control*, 52(8):1362–1379, August 2007.

A. P. Aguiar, D. B. Dačić, J. P. Hespanha, and P. Kokotović. Path-following or reference-tracking: An answer relaxing the limits to performance. In *th IFAC/EURON Symposium on Intelligent Autonomous Vehicles*, Lisbon, Portugal, July 2004.

A. P. Aguiar, J. P. Hespanha, and P. V. Kokotović. Path-following for nonminimum phase systems removes performance limitation. *IEEE Transactions on Automatic Control*, 50(2):234–239, February 2005a.

A. P. Aguiar, J. P. Hespanha, and P. V. Kokotović. Limits of performance in reference-tracking and path-following for nonlinear systems. *Proc. of 16th IFAC World Congress*, 2005c.

M. Benosman and G. Le Vey. Stable inversion of siso nonminimum phase linear systems through output planning: An experimental application to the one-link flexible manipulator. *IEEE Transactions on Control Systems Technology*, 11(4):5–29, July 2003.

M. Benosman and G. Le Vey. End-effector motion planning for one-link flexible robot. *Symposium on Robot Control*, pages 561–566, September 2000a.

M. Benosman and G. Le Vey. Accurate trajectory tracking of flexible arm end-point. *Symposium on Robot Control*, pages 567–572, September 2000b.

M. Benosman, F. Boyer, G. Le Vey, and D. Primault. Flexible links manipulators: From modelling to control. *International Journal Of Intelligent And Robotics Systems*, 34(4):381–414, 2002.

B. B. Dačić. *Path-Following: an Aternative to Reference Tracking*. PhD thesis, University of California, Santa Barbara, June 2005.

Alberto Isidori. *Nonlinear Control Systems II*. Springer, 1999.

J. Martins, M. A. Botto, and J. Sá da Costa. Modeling of flexible beams for robotic manipulators. *Multibody System Dynamics*, 7:79–100, 2002.

J.M. Martins, Z. Mohamed, M.O. Tokhi, J. Sá da Costa, and M.A. Botto. Approaches for dynamic modelling of flexible manipulator systems. *IEE Proceedings - Control Theory and Applications*, 150(4):401–411, 2003.

J.M. Martins, J. Sá da Costa, and M.A. Botto. Modeling, control and validation of flexible robot manipulators. In *Advances in Computational Multibody Systems*, pages 239–268. Springer-Verlag, 2005.

Pedro Pires. Trajectory control of a single link rigid-flexible manipulator. Master's thesis, Instituto Superior Técnico, September 2007.

R. Skjetne. *The Maneuvering Problem*. PhD thesis, Norwegian University of Science and Technology, Dept. Eng. Cybernetics, Trondheim, Norway, 2005.